Monthly Notices of the ROYAL ASTRONOMICAL SOCIETY

MNRAS **520,** 1659–1671 (2023) https://doi.org/10.1093/mnras/stad205
Advance Access publication 2023 January 19

Structure, spectroscopic signatures, and formation of hydroxy-azirine: a potential interstellar prebiotic molecule

Pilar Redondo,* Miguel Sanz-Novo, Carmen Barrientos and Antonio Largo
Computational Chemistry Group, Departamento de Química Física y Química Inorgánica, Universidad de Valladolid, E-47011 Valladolid, Spain

Accepted 2023 January 17. Received 2023 January 17; in original form 2022 December 6

ABSTRACT

Hydroxy-azirine (C_2H_3NO) is a -OH derivative of azirine (C_2H_3N), molecule that has been the subject of several unfruitful searches in space. Hydroxy-azirine is an isomer of the detected prebiotic species methyl isocyanate, CH_3NCO, and glycolonitrile, $HOCH_2CN$, as well as the yet undetected imine acetaldehyde, NHCHCHO. However, the lack of preliminary spectroscopic data on hydroxy-azirine has prevented its astronomical search. The aim of this study is to provide high-level theoretical spectroscopic signatures of the most stable hydroxy-azirine isomers to enable their eventual interstellar search. A total of 12 isomers have been characterized for hydroxy-azirine and their isomerization processes have been analysed at the CCSD(T)-F12/cc-pVTZ-F12 level. The most stable structures are 3-hydroxy-2H-azirine (I) and 2-hydroxy-2H-azirine (II) in their *syn*- and *anti*-configurations, which are suggested as the most relevant candidates for laboratory and interstellar detection. To ease their identification by means of rotational spectroscopy, we report a set of the required spectroscopic parameters using state-of-the-art composite and coupled-cluster approaches. For astronomical purposes, we provide a complete line list for I-*syn* and I-*anti* hydroxy-azirine up to 50 GHz, which takes the hyperfine structure into account, and will be essential to hunt for these interstellar candidates experimentally. In addition, anharmonic vibrational frequencies and intensities are reported to predict a trustworthy vibrational spectra and to estimate the vibrational partition function. Finally, we analyse the possibility of formation of hydroxy-azirine from the reaction of azirine with the hydroxyl radical in the gas-phase and on the surface of ices, finding for the latter a feasible formation route under interstellar conditions.

Key words: astrochemistry – astrobiology – molecular data – molecular processes – ISM:molecules – ISM:general.

1 INTRODUCTION

Among the ∼270 molecules that are currently detected in the interstellar medium or circumstellar shells, the so-called interstellar complex organic molecules (iCOMs) (organic molecules containing more than six atoms) (McGuire et al. 2018; McGuire 2022) are of fundamental interest to astrobiology since these molecules are at the foundation of interstellar prebiotic chemistry. Within this framework, in the last years pure aromatic hydrocarbons or functionalized aromatic molecules, where a hydrogen atom of the ring is replaced by a cyano or ethynyl radical, have been identified in the QUIJOTE (Q-band Ultrasensitive Inspection Journey to the Obscure TMC-1 Environment) and the GOTHAM (GBT Observations of TMC-1: Hunting Aromatic Molecules) line surveys of the cold pre-stellar core Taurus Molecular Cloud 1 (TMC-1) (for a list of detected molecules see Cernicharo et al. (2021a), and references therein). Heterocycles are a related class of cyclic molecules, where at least a CH unit in a carbon ring is replaced by a heavier heteroatom (i.e. N, O, Si, or S). Diverse O-bearing heterocycles, such as oxirane (Dickens et al. 1997), 2-methyloxirane (McGuire et al. 2016), and furan (Kutner et al. 1980) were characterized towards Sagittarius B2 (Sgr B2), whereas in IRC + 10216 the Si-bearing species, silicon dicarbide (Thaddeus et al. 1984) and silicon tricarbide (Apponi et al. 1999) have been detected.

Of particular relevance from a biological point of view are the N-heterocycles. They form the backbone of nucleo-bases, which constitute the subunits assembling the DNA and RNA and they are components of the co-factors of enzymes (Peeters et al. 2003, 2005; Rodriguez et al. 2019). Several nitrogen heterocycles, such as pyridine carboxylic acids, purines, pyrimidines, triazines, pyridines, quinolines, carboxylactams, or proline, have been detected in carbonaceous meteorites (Martins 2018), but, to date, no nitrogen-containing heterocycle has been conclusively detected in the interstellar medium (ISM). The simplest N-heterocyclic compounds, 2H-Azirine, c-C_2H_3N, and aziridine (ethylenimine), c-C_2H_5N, have been the subject of several searches without a conclusive identification. A tentative detection of aziridine was carried out by Dickens et al. (2001) towards several hot cores, including Sgr B2(N). Both, aziridine and 2H-azirine, have been the target of several searches toward the hot core Orion KL and W51 e1/e2 (Kuan et al. 2004), and lately Barnum et al. (2022) were not able to detect them towards TMC-1. A recent experimental and computational study shows the detection and formation of ethynamine ($HCCNH_2$) and 2H-azirine (c-C_2H_3N) by irradiating with electrons ices of ammonia and acetylene that simulate interstellar ices processed by galactic cosmic rays (Turner et al. 2021).

Hydroxy-azirine, with molecular formula C_2H_3NO, is a functionalized derivative of azirine (c-C_2H_3N), where a hydrogen atom

* E-mail: pilar.redondo@uva.es

is replaced by a -OH unit. Hydroxy-azirine is an isomer of the detected prebiotic species methyl isocyanate, CH_3NCO, (Halfen, Ilyushin & Ziurys 2015) and glycolonitrile, $HOCH_2CN$, (Zeng et al. 2019). Methyl isocyanate may be involved in the formation of peptide-bond-like molecules such as methyl-formamide, by successive hydrogenation processes (Belloche et al. 2017). The relevance of glycolonitrile in prebiotic chemistry is related to its role as a possible precursor of glycine (Rodriguez et al. 2019), and it also is a key intermediate in the formation of adenine (Schwartz, Joosten & Voet 1982; Menor-Salván & Marín-Yaseli 2012). In addition, imino acetaldehyde, NHCHCHO, another isomer of hydroxy-azirine, was suggested as a possible interstellar molecule (Redondo, Largo & Barrientos 2018). Today, different isomers containing different functional groups, such as acetaldehyde (CH_3CHO) (Gottlieb 1973), ethylene oxide (c-C_2H_4O) (Dickens et al. 1997), and vinyl alcohol (CH_2CHOH) (Turner & Apponi 2001), have been identified toward Sagittarius B2(N). For some isomeric families, the most stable isomer is also the most abundant one in the ISM, in accordance with the Minimum Energy Principle, MEP (Lattelais et al. 2009). Nevertheless, discrepancies of this principle may be observed since the formation routes could be different and, the kinetic factors will be key to rationalize their abundances. The identification, abundances, and spatial distribution of different isomers shall be useful to understand their formation routes and the overall evolution of prebiotic molecules. On the other hand, a recent theoretical study shows a protonated derivative of hydroxy azirine as a possible product the reaction between HNO and $CH_2CHOH_2^+$ under interstellar conditions (Redondo et al. 2017).

In this work we present a high-level computational study of hydroxy-azirine (c-C_2H_3NO), a reasonable interstellar candidate. The main aim is to provide a high-level calculated array of the relevant spectroscopic parameters to rotational and infrared (IR) spectroscopy for the most stable isomers of hydroxy-azirine to facilitate their eventual spectral searches. Nowadays, the availability of radio telescopes with outstanding bandwidth, sensitivity, and resolution, and the implementation of new experimental techniques has opened the door to a vast amount of new and very sensitive astronomical data (Cernicharo et al. 2021b,c; Loomis et al. 2021; Lee et al. 2021) which are awaiting for new detections. To do this, previous theoretical or experimental spectroscopic characterization of possible candidates is crucial to achieve conclusive interstellar detection.

We will characterize isomers and conformers of hydroxy-azirine (c-C_2H_3NO), with the so-called 'spectroscopic' accuracy, employing a composite approach (Redondo et al. 2018; Redondo et al. 2020). Relevant spectroscopic signatures for rotational and infrared spectroscopy are also provided for the most stable species, which will be needed to guide an eventual laboratory or interstellar detection. In addition, we will also analyse the formation of hydroxy-azirine from azirine in the gas phase and on the surface of ices.

2 COMPUTATIONAL METHODS

Ab initio and density functional theory (DFT) methodologies were employed for the study of hydroxy-azirine (c-C_2H_3NO). We first characterized their isomers and conformers at the DFT level using the double hybrid B2PLYPD3 functional (Grimme 2006). This functional includes Hartree-Fock exchange and a perturbative second-order correlation part, combined with the Grimme's D3BJ empirical dispersion term (Grimme, Ehrlich & Goerigk 2011). For these calculations we have used the Dunning's correlation consistent triple-zeta basis sets, aug-cc-pVTZ (Dunning 1989; Woon & Dunning 1993), which also includes both polarization and diffuse functions on all elements. In a second step, more precise structural parameters and energies were computed at the explicitly correlated (F12) coupled cluster level including singles, doubles, and perturbative triplet excitations (CCSD(T)-F12 method) (Knizia, Adler & Werner 2009) in conjunction with the cc-pVTZ-F12 basis set (Peterson, Adler & Werner 2008). On each stationary point, harmonic vibrational frequencies were calculated at the B2PLYPD3 and CCSD(T)-F12 levels to characterize them as minima (all real frequencies) or transition state structures (one imaginary frequency), and estimate their zero point vibrational energy (ZPVE). To validate our single reference calculations, we have calculated the T1 diagnostic (Lee & Taylor 1989) at the CCSD(T) level (Raghavachari et al. 1989). For all the structures considered, the T1 diagnostic is around 0.013, showing the viability of our single reference calculations. Note that a T1 diagnostic lower than 0.02 implies that single reference methods may give reliable predictions (Lee & Taylor 1989).

To obtain more accurate rotational constants, a composite procedure (Gardner et al. 2021) was also applied for the most relevant isomers. Composite approaches are based on the assumption that an estimated property can be obtained as a sum of additive contributions and have been previously employed in similar systems (Redondo et al. 2018; Redondo et al. 2020). In this work, composite parameters are estimated using two different schemes. In the first one we took as reference the *ab initio* CCSD(T) method with the aug-cc-pVTZ basis sets (Dunning 1989; Woon & Dunning 1993) and the geometrical parameters or rotational equilibrium constants, denoted as P1(comp), are calculated as:

$$P1(comp) = P1(CBS) + \Delta P(CV). \quad (1)$$

where P1(CBS) corresponds to the complete basis set (CBS) limit extrapolated value that considers basis-set truncation errors. It is computed from the n^{-3} extrapolation equation (Helgaker et al. 1997) applied to the cases of $n = 3$ (T) and $n = 4$ (Q), that is using CCSD(T)/aug-cc-pVTZ and CCSD(T)/aug-cc-pVQZ data, respectively. The term ΔP(CV), accounts for core-valence (CV) effects. It is calculated taking the difference between a calculation including all electrons (ae) and a frozen-core (fc) approach:

$$\Delta P(CV) = P(ae - CCSD(T)/cc - pCVTZ) - P(fc - CCSD(T)/cc - pCVTZ). \quad (2)$$

In the second composite approach, denoted as P2(comp), parameters are estimated:

$$P2(comp) = P2(CBS) + \Delta P(CV) + \Delta P(aug) \quad (3)$$

the CCSD(T)/cc-pVTZ level is took as reference, the complete basis set (CBS) limit extrapolated parameter is computed using the basis set cc-pVTZ and cc-pVQZ and the effect of diffuse function in the bases is considered by the term:

$$\Delta P(aug) = P(CCSD(T)/aug - cc - pVTZ) - P(CCSD(T)/cc - pVTZ) \quad (4)$$

The corresponding composite energies include the ZPVE term estimated at the CCSD(T)/aug-cc-pVTZ within the anharmonic approach.

To predict the IR spectra with sufficient accuracy to be useful for spectroscopists in a possible laboratory identification, anharmonic corrections are estimated for the most stable isomers at the CCSD(T)/aug-cc-pVTZ level of theory using the second-

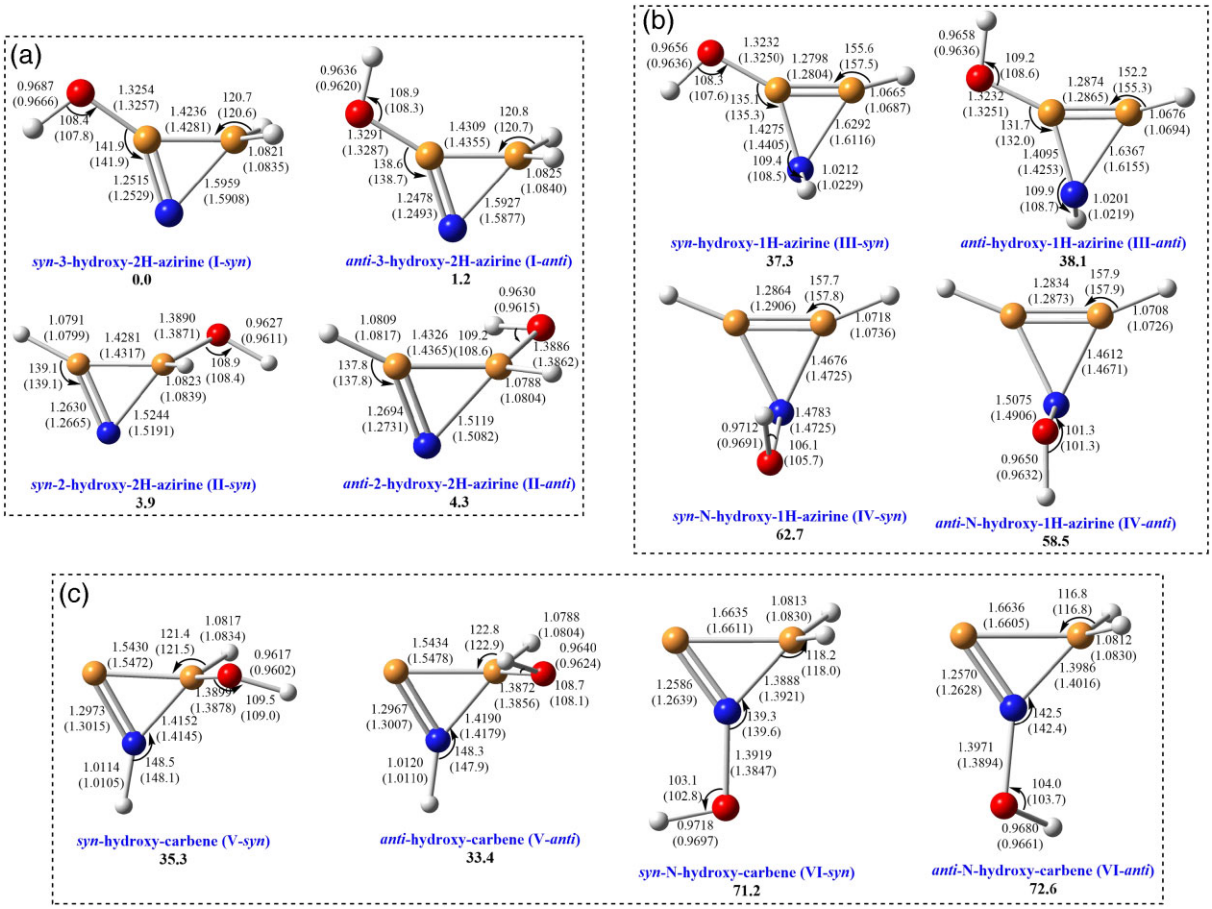

Figure 1. Optimized geometrical parameters of the isomers and conformers located for the three isomeric families of hydroxy-azirine (in angstroms and degrees) obtained at the B2PLYPD3/aug-cc-pVTZ and CCSD(T)-F12/cc-pVTZ-F12 (in parentheses). Relative energies in kcal/mol computed at the CCSD(T)-F12/cc-pVTZ-F12 level (ZPV energies included).

order vibrational perturbation theory (VPT2) (Mills 1972) within the context of the Watson Hamiltonian (Watson 1968). A full cubic force field (CFF) and semidiagonal quartic force constants have been included in the procedure. From the CFF calculations, we have computed vibration-rotation interaction constants. Moreover, this information should be of interest to adequately determine the vibrational contribution (Q_v) to the total partition function (Q_{tot}), which is required to achieve a proper estimation of the total column density (upper limit) of a molecule in the ISM.

Quantum calculations are carried out using methods as implemented in the GAUSSIAN 16 program package (Frisch et al. 2016), MOLPRO (Werner et al. 2019), and the CFOUR Program (Stanton et al. 2013).

3 RESULTS AND DISCUSSION

In this section, we will start with a discussion of the structures and stability of the located hydroxy-azirine isomers; conformers of each isomer are also considered. Then we will analyze the different interconversion processes between isomers and conformers. For the most stable structures, spectroscopic parameters are reported to help in their experimental characterization. Finally, a brief discussion of plausible formation processes is presented.

3.1 Structure and stability of the hydroxy-azirine isomers and conformers

As we have commented in Section 1, the main objective of this work is to characterize the different structures of the potential interstellar species, hydroxy-azirine (c-C_2H_3NO) that can be seen as a OH derivative of the nitrogen-containing three members cycle azirine (C_2H_3N). The geometrical parameters of the different hydroxy-azirine structures located on the singlet potential energy surface, computed with the B2PLYPD3 and the CCSD(T)-F12 methods, are shown in Fig. 1. Taking as reference the theoretical study of Dickerson et al. (Dickerson, Bera & Lee 2018), where they characterize the three isomers of azirine, named 2H-azirine, carbene isomer (1H,2,2H-azirine), and 1H-azirine, we have classified the structures of hydroxy-azirine in three groups or isomeric families, depending on the azirine structure from which they are derived. Therefore, in part a) of Fig. 1 we display the isomers, 3-hydroxy-2H-azirine and 2-hydroxy-2H-azirine, denoted as isomer I and II, which arise from 2H-azirine. For each isomer we have characterized two conformers which differ in the orientation of the OH group, and we will denote them as *syn-* and *anti-*. The substitution of one of the hydrogens by the hydroxyl group in 1H-azirine leads also to two isomers, hydroxy-1H-azirine (isomer III) and N-hydroxy-1-H-azirine (isomer IV), which, as in the previous case, present two different *syn-* and *anti-* conformations (see Fig. 1b). Similarly, for the third isomer of azirine, the carbene-like, we have found two isomers, hydroxy-carbene

(isomer V) and N-hydroxy-carbene (isomer VI), characterizing for each of them the conformers *syn*- and *anti*-, as can be seen in part c) of Fig. 1. For the 12 hydroxy azirine structures, in Table 1 we report their relative energies, equilibrium rotational constants and dipole moment components. In addition, as Supplementary Material (online), we report their geometries and harmonic vibrational frequencies computed at the B2PLYPD3/aug-cc-pVTZ and CCSD(T)-F12/cc-pVTZ-F12 levels.

When we analyse the geometrical parameters shown in Fig. 1, we can observe that, in general, the results obtained at both levels of theory, B2PLYPD3/aug-cc-pVTZ and CCSD(T)-F12/cc-pVTZ-F12, are very close; the differences in the calculated bond distances are of the order of thousandths of angstroms and less than one degree for the angles. The differences obtained for the bond distances and angles between the *syn*- and *anti*- conformers are very small, and the main discrepancy between them is found in the dihedral angle formed by the hydrogen atom of the hydroxyl group. If we compare our computed geometries of the hydroxy-azirine isomers with those obtained by Dickerson et al. (2018) for azirine, we can see that the substitution of one hydrogen atom of azirine by the hydroxyl group does not produce significant changes in the corresponding geometrical parameters. For instance, the C–N and C–C bond distances obtained for isomers I and II have the same character than that found in 2H-azirine, i.e. one C–N bond is an elongated single bond, the other is between double and triple bond, and the C–C is a single bond with slightly double character. Finally, we will compare the geometries calculated for the isomers arising from the corresponding isomers of azirine. The difference observed between the geometrical parameters of isomer I and II, both derived from 2H-azirine, is that there is a slight decrease in the C–N bond distance of the carbon attached to the hydroxyl group. If we compare isomers III and IV, originated from 1H-azirine, we observe that for isomer III the C–N distance of the carbon attached to the hydroxyl is shortened and the other C–N distance is lengthened, with respect to isomer IV. In the carbene-derived isomers, when the hydroxyl is attached to the nitrogen isomer IV the C–N bond distances are slightly shorter than the corresponding ones of isomer V, whereas the C–C bond distance is slightly lengthened.

The variations found in the geometrical parameters of the characterized structures are reflected in the calculated values of the equilibrium rotational constants shown in Table 1. As can be seen, the two distinct conformers of an isomer have very similar constants, but there is a sizable change in the dipole moment components, which will be translated in notorious differences in their rotational spectra.

The stability order of the hydroxy-azirine isomers and conformers calculated with the B2PLYPD3 and CCSD(T)-F12 methods is the same, and the energy differences computed at both levels differ by less than 1 kcal/mol. Note that the largest discrepancies are found for isomers II and V, where the differences are in the order of 1 kcal/mol (see Table 1). In their study of azirine isomers, Dickerson et al. (2018) obtained that the most stable isomer is 2H-azirine, with the carbene isomer and 1H-azirine located at 29.8, and 33.5 kcal/mol at the CCSD(T)/cc-pV5Z level, respectively, order that nicely agrees with that found in previous studies on azirine (Tavakol 2010; Csaszar, Demaison & Rudolph 2015). Hydroxy-azirine isomers derived from the more stable azirine isomer, 2H-azirine, are also the most stable ones. In particular, the isomer 3-hydroxy-2H-azirine in its *syn*-conformation (I-*syn*) is the lowest-lying. The corresponding *anti*-conformer (I-*anti*) is located only 1.21 kcal/mol above I-*syn* at the CCSD(T)-F12/cc-pVTZ-F12 level. The next isomer in stability is 2-hydroxy-2H-azirine, the *syn*- and *anti*-conformers lie 3.86 and 4.26 kcal/mol from the I-*syn* isomer at the CCSD(T)-F12/cc-pVTZ level, respectively. For isomers arising from the carbene azirine isomer and H-azirine, we have found that when the hydroxyl is bonded to the carbon atom, they are much more stable than when the bond is formed on the nitrogen one. Thus, we obtain that *syn*-hydroxy-carbene (V-*syn*) and *syn*-N-hydroxy-carbene (VI-*syn*) are located 35.30 and 71.24 kcal/mol above I-*syn* at CCSD(T)-F12/cc-pVTZ-F12 level, respectively. As in azirine, the isomers derived from the carbene-like isomer are more stable than those from 1H-azirine when the -OH substitution takes place at the carbon (*anti*-hydoxy-carbene is most stable than *anti*-hydroxy-1H-azirine), but if it is substituted at the nitrogen, the order is reversed (*anti*-N-hydoxy-carbene is less stable than *anti*-N-hydroxy-1H-azirine) (see Table 1 and Fig. 1). Regarding the stability between conformers, we have found that the *syn*-conformers are slightly more stable than the *anti*-conformers, except for the hydroxy-carbene and N-hydroxy-1H-azirine isomers.

At both levels of theory, the order of stability obtained for the hydroxy-azirine isomers is as follows (> means more stable than): I-*syn* > I-*anti* > II-*syn* > II-*anti* > V-*anti* > V-*syn* > III-*syn* > III-*anti* > IV-*anti* > IV-*syn* > VI-*syn* > VI-*anti*

In order to obtain more accurate structural parameters and energies we have carried out high level ab initio calculations for the four most stable isomers, which will be the most relevant from an experimental point of view. Specifically, we have employed composite approaches, as described in Section 2. The geometrical parameters and the relative energies for the two conformers of 3-hydroxy-2H-azirine, computed at different levels of theory, are shown in Table 2, and those corresponding to the 2-hydroxy-2H-azirine conformers are reported in Table 3. If we compare the structural results, we observe that the inclusion of corrections at the composite levels for core-valence effect and incompleteness of the basis set is needed to obtain accurate structures. The two composite approximations used, denoted as P1 and P2, differ in the way of including diffuse functions. In the P2 approximation they are taken into account as a contribution, while in the P1 scheme the diffuse functions are included in the bases. The results obtained with the two composite approximations employed are very close, as it can be seen in Table 2. Therefore, for the 2-hydroxy-2H-azirine conformers (Table 3) only the P2 approximation has been employed. Regarding the relative energies, as shown in Tables 2 and 3, the stability order is maintained regardless of the level employed, although the energy difference between conformers is very small. The stability difference between the two 3-hydroxy-2H-azirine conformers is 1.18 kcal/mol at the P1 composite level, and that calculated between the 2-hydroxy-2H-azirine conformers is only 0.42 kcal/mol at the P2 composite level.

3.2 Interconversion processes between hydroxy-azirine structures

In this section, we will analyze the isomerization processes between the twelve structures characterized for hydroxy-azirine. First, we will study the interconversion between the *syn*- and *anti*-conformers of each of the isomers to check whether severe relaxation processes may occur or not. The corresponding *syn-anti* rotation barriers, V(*syn/anti*), are collected in Table 4. Prior to optimizing the transition states that connect the two conformers, we performed a scan that bridge both conformers by varying the $\angle CCOH$ dihedral angle, which changes the orientation of hydroxyl (-OH) group. The results obtained for the 3-hydroxy-2H-azirine (I) and 2-hydroxy-2H-azirine (II) isomers are shown in Fig. 2. When the rotation of the hydroxyl group is not symmetric in both directions, two values of the interconversion barrier are obtained, as can be seen in the relaxed

Table 1. Relative energies including ZPV energies in kcal/mol and eV (in parentheses), rotational constants in MHz, and dipole moment components in Debye for the isomers and conformers of hydroxy-azirine.

	Method	ΔE	A	B	C	μ_x	μ_y	μ_z
I-*syn*	B2PLYPD3	0.00(0.00)	23920.96	7550.89	5970.65	1.29	−0.73	0.00
	CCSD(T)-F12	0.00(0.00)	24078.15	7510.50	5956.32			
I-*anti*	B2PLYPD3	1.28(0.06)	23850.81	7519.20	5946.39	1.11	−3.57	0.00
	CCSD(T)-F12	1.21(0.05)	23985.75	7484.47	5934.24			
II-*syn*	B2PLYPD3	4.88(0.21)	25373.92	7264.99	6653.81	−0.32	0.85	-1.29
	CCSD(T)-F12	3.86(0.17)	25236.07	7295.03	6673.87			
II-*anti*	B2PLYPD3	5.33(0.23)	25120.89	7217.24	6726.37	0.78	2.16	0.51
	CCSD(T)-F12	4.26(0.18)	24999.08	7244.75	6747.95			
III-*syn*	B2PLYPD3	37.44(1.62)	21996.26	7783.77	5873.60	−0.82	−0.46	0.89
	CCSD(T)-F12	37.29(1.62)	22340.30	7687.27	5839.35			
III-*anti*	B2PLYPD3	38.10(1.65)	22005.15	7804.14	5891.76	−1.26	2.24	−0.68
	CCSD(T)-F12	38.10(1.65)	22422.67	7690.61	5850.62			
IV-*syn*	B2PLYPD3	63.43(2.75)	21852.24	7820.78	7007.09	−3.00	0.00	−2.27
	CCSD(T)-F12	62.72(2.72)	21722.24	7885.01	7051.77			
IV-*anti*	B2PLYPD3	58.97(2.56)	22109.94	7773.00	6953.17	1.39	0.00	−0.11
	CCSD(T)-F12	58.47(2.54)	22033.92	7838.97	6994.62			
V-*syn*	B2PLYPD3	36.58(1.59)	25190.97	7327.34	6707.84	−0.67	−4.12	1.45
	CCSD(T)-F12	35.30(1.53)	25027.50	7344.63	6714.96			
V-*anti*	B2PLYPD3	34.71(1.51)	24658.71	7357.15	6774.81	0.41	−2.13	−0.28
	CCSD(T)-F12	33.35(1.45)	24504.51	7376.67	6786.94			
VI-*syn*	B2PLYPD3	71.61(3.11)	23140.38	7749.42	6046.02	1.13	−1.13	0.00
	CCSD(T)-F12	71.24(3.09)	23162.92	7752.02	6050.34			
VI-*anti*	B2PLYPD3	72.96(3.16)	23006.14	7673.60	6032.84	−0.86	−3.67	−0.80
	CCSD(T)-F12	72.65(3.15)	23018.46	7678.62	6045.10			

potential energy surface (PES) scan Fig. 2 (b). Note that the lowest barrier is included in Table 4.

The highest energetic rotation barrier, 5.17 kcal/mol (≈ 2600 K) at the CCSD(T)-F12/cc-pVTZ-F12 level, is found for the most stable isomer, 3-hydroxy-2H-azirine (I). Regarding an eventual experimental study, it is well established that for jet-cooled experiments conformational relaxation processes can transpire through collisions with the carrier gas if interconversion barriers are low enough (about 1.15 kcal/mol or 400 cm^{-1} and lower) (Ruoff et al. 1990; Miller, Clary & Meijer 2005). Therefore, both I-*syn* and I-*anti* conformers can be identified experimentally in the laboratory and also in the ISM. For the second isomer in stability, 2-hydroxy-2H-azirine (II), a barrier of 0.25 kcal/mol (≈ 125 K or 87 cm^{-1} at the CCSD(T)-F12/cc-pVTZ-F12 level) is obtained, indicating that both *syn*- and *anti*-conformers could be present in low-temperature interstellar clouds. Moreover, the extremely low-energy predicted V(*syn/anti*) barrier allow us to anticipate the absence of conformer II-*anti* in an eventual jet-cooled experiment. The lowest barrier, 0.04 kcal/mol (≈ 20 K), is found for hydroxy carbene (V) at the CCSD(T)-F12/cc-pVTZ-F12. In this isomer the conversion from V-*syn* to V-*anti* conformer will take place, unless temperatures are extremely low. The energetic barrier for N-hydroxy carbene is slightly higher (≈ 85 K at the CCSD(T)-F12/cc-pVTZ-F12 level) and only in cool regions could be present both conformers. For the two isomers of 1H-azirine, the lowest barrier is found for N-hydroxy-1H-azirine (≈ 320 K at the CCSD(T)-F12/cc-pVTZ-F12 level).

We will now study the isomerization processes between the different hydroxy-azirine isomers, considering also the formation of linear species by breaking the cycle. As we can see in Table 5, both levels of theory, B2PLYPD3/aug-cc-pVTZ and CCSD(T)-F12/cc-pVTZ-F12, employed for the determination of the interconversion barriers give very close results. Therefore, the study of isomerization processes has been carried out at the B2PLYPD3/aug-cc-pVTZ level, and the obtained results are shown in Fig. 3. All the isomerization processes considered involve significant activation barriers, which implies that interconversion between isomers would not be possible in the interstellar medium, and if viable formation pathways exist the different isomers could be indeed present. For instance, if we consider the *syn*-2-hydroxy-2H-azirine (II-*syn*) isomer, the barrier for isomerization to the more stable isomer, *syn*-3-hydroxy-2H-azirine, is 54.7 kcal/mol, and the formation of the open-chain HNCCHOH, which is an exothermic process, involves a transition state located 50.0 kcal/mol above II-*syn*.

3.3 Spectroscopic parameters for laboratory or astronomical detection

With the aim of hunting for the most stable hydroxy-azirine structures (I-*syn*, I-*anti*, II-*syn*, and II-*anti*) in the laboratory or in the ISM eventually by means of rotational spectroscopy, we provide a complete theoretical set of their relevant rotational spectroscopic parameters to ease future spectral searches. Firstly, we report in Table 5 the equilibrium rotational constants, calculated using the aforementioned composite approach, along with the ground state rotational constants. The latest were computed by taking the vibrational correction into account, which is obtained from the vibration-rotation coupling constants [calculated from the full anharmonic cubic force field, CFF)] and degeneracy factors of the vibrational modes. Moreover, we report the ^{14}N nuclear quadrupole coupling constants calculated at the CCSD/aug-cc-pVTZ using the composite geometry, along with the CCSD(T)/aug-cc-pVTZ calculated quartic centrifigal distortion parameters, to fully reproduce the rotational spectra. In particular, the hyperfine structure (HPS) is crucial to enable a secure line-by-line detection of N-bearing molecules using different centimetre-wave line surveys (see for instance the detection of N-protonated isocyanic acid, H_2NCO^+, toward the molecular cloud G + 0693-0.027 (Rodríguez-Almeida et al. 2021)).

Table 2. Structural parameters (distances in Angstroms and angles in degrees) and relative energies (ZPV energies included) in kcal/mol for the 3-hydroxy-2H-azirine conformers at different levels of theory.

	$C_1N^{(a)}$	C_2N	C_1C_2	C_1O	C_2H	OH	$<OC_1N$	$<C_1C_2H$	$<HOC_1$	$<NC_1C_2H$	ΔE
syn-3-hydroxy-2H-azirine (I-syn)											
CCSD(T)-F12/cc-pVTZ-F12	1.2529	1.5908	1.4281	1.3257	1.0835	0.9666	141.9	120.6	107.8	98.5	0.00
CCSD(T)/cc-pVTZ	1.2566	1.5972	1.4312	1.3294	1.0841	0.9677	142.0	120.6	107.3	98.6	0.00
CCSD(T)/cc-pVQZ	1.2529	1.5908	1.4282	1.3259	1.0834	0.9658	141.9	120.6	107.7	98.6	0.00
ae-CCSD(T)/cc-pCVTZ	1.2532	1.5927	1.4280	1.3266	1.0830	0.9665	142.1	120.6	107.4	98.6	0.00
CCSD(T)/aug-cc-pVTZ	1.2569	1.5984	1.4317	1.3300	1.0847	0.9691	141.9	120.6	107.6	98.5	0.00
CCSD(T)/aug-cc-pVQZ	1.2534	1.5922	1.4287	1.3264	1.0836	0.9665	141.9	120.6	107.8	98.5	0.00
P2(composite)	1.2483	1.5833	1.4242	1.3219	1.0823	0.9651	141.8	120.6	108.4	98.6	0.00
P1(composite)	1.2487	1.5837	1.4242	1.3216	1.0818	0.9639	141.9	120.6	108.1	98.6	0.00
anti-3-hydroxy-2H-azirine (I-anti)											
CCSD(T)-F12/cc-pVTZ-F12	1.2493	1.5877	1.4355	1.3287	1.0840	0.9620	138.7	120.7	108.3	98.3	1.21
CCSD(T)/cc-pVTZ	1.2531	1.5944	1.4384	1.3327	1.0846	0.9631	138.8	120.8	107.6	98.4	1.31
CCSD(T)/cc-pVQZ	1.2493	1.5879	1.4354	1.3290	1.0839	0.9613	138.8	120.7	108.1	98.4	1.21
ae-CCSD(T)/cc-pCVTZ	1.2497	1.5899	1.4354	1.3298	1.0834	0.9620	138.9	120.8	107.8	98.4	1.31
CCSD(T)/aug-cc-pVTZ	1.2533	1.5955	1.4390	1.3331	1.0851	0.9645	138.7	120.7	108.1	98.2	1.15
CCSD(T)/aug-cc-pVQZ	1.2498	1.5891	1.4360	1.3293	1.0841	0.9619	138.7	120.7	108.3	98.3	1.16
P2(composite)	1.2446	1.5805	1.4316	1.3245	1.0827	0.9606	138.7	120.7	109.1	98.4	0.99
P1(composite)	1.2451	1.5806	1.4314	1.3244	1.0823	0.9593	138.8	120.7	108.6	98.4	1.18

Note.$^{(a)}$ C_1 denotes the carbon atom bonded to the oxygen.

Table 3. Structural parameters (distances in Angstroms and angles in degrees) and relative energies (ZPV energies included) in kcal/mol for the 2-hydroxy-2H-azirine conformers at different levels of theory.

	$C_1N^{(a)}$	C_2N	C_1C_2	C_1O	C_2H	C_2H	OH	$<OC_1C2$	$<NC_2H$	$<HC_1C_2$	$<HOC_1$	$<OC_1C_2N$	$<HC_1C_2N$	$<C_2C_1OH$	$\Delta E^{(b)}$
syn-2-hydroxy-2H-azirine (II-syn)															
CCSD(T)-F12/cc-pVTZ-F12	1.5192	1.2665	1.4317	1.3872	1.0839	1.0799	0.9611	118.4	139.2	122.4	108.4	103.9	−99.2	−146.5	3.86
CCSD(T)/cc-pVTZ	1.5273	1.2706	1.4354	1.3885	1.0843	1.0804	0.9623	118.6	139.1	122.1	107.7	104.1	−99.0	−144.5	4.48
CCSD(T)/cc-pVQZ	1.5207	1.2666	1.4320	1.3864	1.0837	1.0797	0.9605	118.5	139.2	122.3	108.2	103.9	−99.1	−145.5	4.05
ae-CCSD(T)/cc-pCVTZ	1.5236	1.2670	1.4322	1.3859	1.0832	1.0796	0.9611	118.6	139.2	122.0	107.8	104.1	−99.0	−144.4	4.63
CCSD(T)/aug-cc-pVTZ	1.5259	1.2709	1.4357	1.3913	1.0847	1.0810	0.9637	118.5	139.2	122.4	108.2	103.9	−99.2	−145.9	3.83
P2(composite)	1.5112	1.2617	1.4277	1.3857	1.0825	1.0786	0.9598	118.3	139.3	122.8	109.2	103.7	−99.4	−147.7	3.17
anti-2-hydroxy-2H-azirine (II-anti)															
CCSD(T)-F12/cc-pVTZ-F12	1.5082	1.2731	1.4365	1.3862	1.0804	1.0817	0.9615	123.3	137.8	123.3	108.6	102.0	−100.8	−24.1	4.26
CCSD(T)/cc-pVTZ	1.5154	1.2778	1.4395	1.3880	1.0808	1.0823	0.9625	123.6	137.8	123.0	107.9	102.3	−100.7	−23.3	4.96
CCSD(T)/cc-pVQZ	1.5088	1.2735	1.4364	1.3859	1.0802	1.0815	0.9607	123.4	137.8	123.2	108.4	102.1	−100.8	−24.1	4.50
ae-CCSD(T)/cc-pCVTZ	1.5117	1.2741	1.4363	1.3854	1.0798	1.0816	0.9613	123.6	137.8	123.0	108.0	102.3	−100.7	−23.5	5.11
CCSD(T)/aug-cc-pVTZ	1.5141	1.2777	1.4401	1.3907	1.0814	1.0828	0.9641	123.4	137.9	123.3	108.4	102.0	−100.8	−24.4	4.29
P2(composite)	1.4997	1.2680	1.4325	1.3850	1.0793	1.0803	0.9603	123.0	138.0	123.6	109.3	101.8	−101.0	−25.8	3.59

Note.$^{(a)}$ C_1 denotes the carbon atom bonded to the oxygen. $^{(b)}$ relative energies with respect to *syn*-3-hydroxy-2H-azirine isomer.

Table 4. Conformer interconversion barriers at the B2PLYPD3/aug-cc-pVTZ and CCSD(T)-F12/cc-pVTZ-F12 levels, in kcal/mol and eV (in parentheses). ZPV energies calculated at each level are included.

Interconversion process	B2PLYPD3	CCSD(T)-F12
anti-3-hydroxy-2H-azirine (I-*anti*) → *syn*-3-hydroxy-2H-azirine (I-*syn*)	5.44 (0.236)	5.17 (0.224)
anti-2-hydroxy-2H-azirine (II-*anti*) → *syn*-2-hydroxy-2H-azirine (II-*syn*)	0.34 (0.015)	0.25 (0.011)
anti-Hydroxy-1H-azirine (III-*anti*) → *syn*-Hydroxy-1H-azirine (III-*syn*)	3.77 (0.164)	3.21 (0.139)
syn-N-hydroxy-1H-azirine (IV-*syn*) → *anti*-N-hydroxy-1H-azirine (IV-*anti*)	0.65 (0.028)	0.64 (0.028)
syn-hydroxy-carbene (V-*syn*) → *anti*-hydroxy-carbene (V-*anti*)	0.03 (0.001)	0.04 (0.002)
anti-N-hydroxy-carbene (VI-*anti*) → *syn*-N-hydroxy-carbene (VI-*syn*)	0.29 (0.012)	0.17 (0.007)

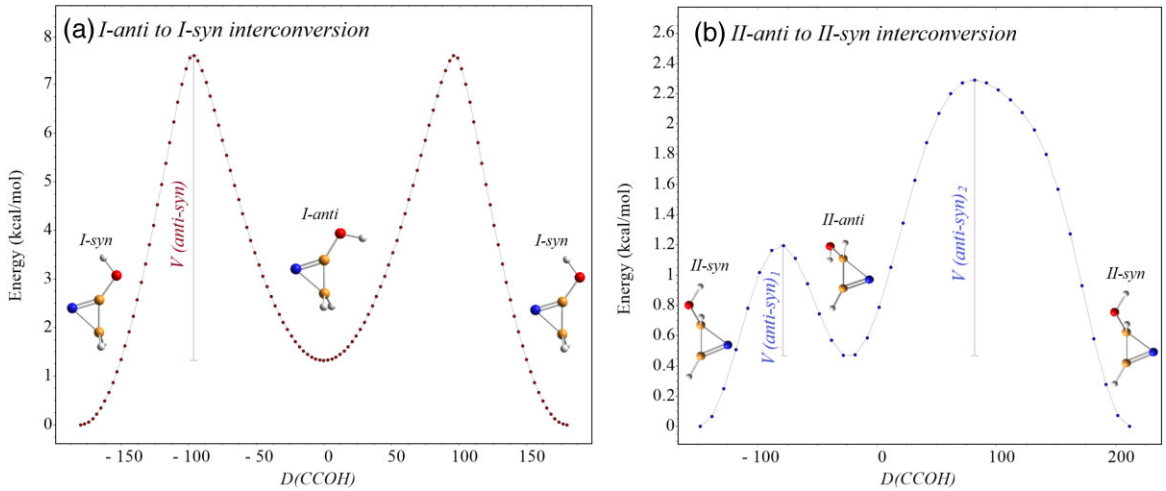

Figure 2. a) Relaxed PES scan computed for the I-*anti* conformer of hydroxy-azirine at the B2PLYPD3/aug-cc-pVTZ level, choosing the ∠*CCOH* torsion (in degrees) as the driving coordinate. b) Relaxed PES scan computed for the II-*anti* conformer at the B2PLYPD3/aug-cc-pVTZ level, choosing the ∠*CCOH* torsion (in degrees) as the driving coordinate.

Table 5. Theoretical equilibrium (*A*, *B*, and *C*) rotational constants computed at the composite level and ground-state (A_0, B_0, and C_0) rotational constants at the CCSD(T)/aug-cc-pVTZ level for I-*syn*, I-*anti*, II-*syn*, and II-*anti* hydroxy-azirine isomers (*S*-Reduction, I^r-Representation). $|\mu_a|$, $|\mu_b|$, $|\mu_c|$ are the absolute values of the electric dipole moment components (in D). χ_{aa}, χ_{bb}, χ_{cc} are the diagonal elements of the ^{14}N nuclear quadrupole coupling tensor, computed at the CCSD/aug-cc-pVTZ level.

Parameters	I-*syn*	I-*anti*	II-*syn*	II-*anti*
A (MHz)	24276.5	24180.2	25391.4	25095.0
B (MHz)	7546.2	7521.0	7335.5	7296.0
C (MHz)	5990.0	5968.1	6716.9	6803.9
A_0 (MHz)	23911.3	23831.5	25165.2	24879.8
B_0 (MHz)	7519.3	7492.6	7283.2	7243.2
C_0 (MHz)	5946.6	5925.5	6675.5	6753.8
$\|\mu_a\|$, $\|\mu_b\|$, $\|\mu_c\|$ (D)	1.2 / 0.7 / 0.0	1.0 / 3.5 / 0.0	0.2 / 0.8 / 1.2	0.8 / 2.1 / 0.5
χ_{aa} (MHz)	−0.724	−0.922	1.074	0.957
χ_{bb}-χ_{cc} (MHz)	−0.483	−0.401	−5.312	−5.385
D_J (kHz)	2.07	2.16	3.61	3.92
D_K (kHz)	123	123	49.4	44.8
D_{JK} (kHz)	6.88	5.41	5.88	6.36
d_1 (kHz)	−0.637	−0.675	−0.129	-0.0362
d_2 (kHz)	−0.122	−0.122	−0.00663	0.0443

The ultimate goal of the search for these interstellar candidates is highly conditioned by the accuracy of the spectral predictions. However, the paucity of experimental spectroscopic data of hydroxy-azirine prevent us from evaluating the accuracy estimation for the rest frequencies. Recently, Alessandrini, Gauss & Puzzarini (2018) reported a thorough theoretical study of different iCOMs using related composite schemes. They analyzed systematic errors related to the values of the rotational constants (i.e. deviations of approximately ∼4 MHz are estimated for thioxoethenylidene, CCS, at very low frequencies). We can, therefore, infer upper limit errors of ∼0.04 per cent in the values of the rotational constants, when stacked up with our predictions in the centimeter-wave region, if we consider that the uncertainties described in Alessandrini et al. (2018) can be transportable to our systems. This is transcribed in an

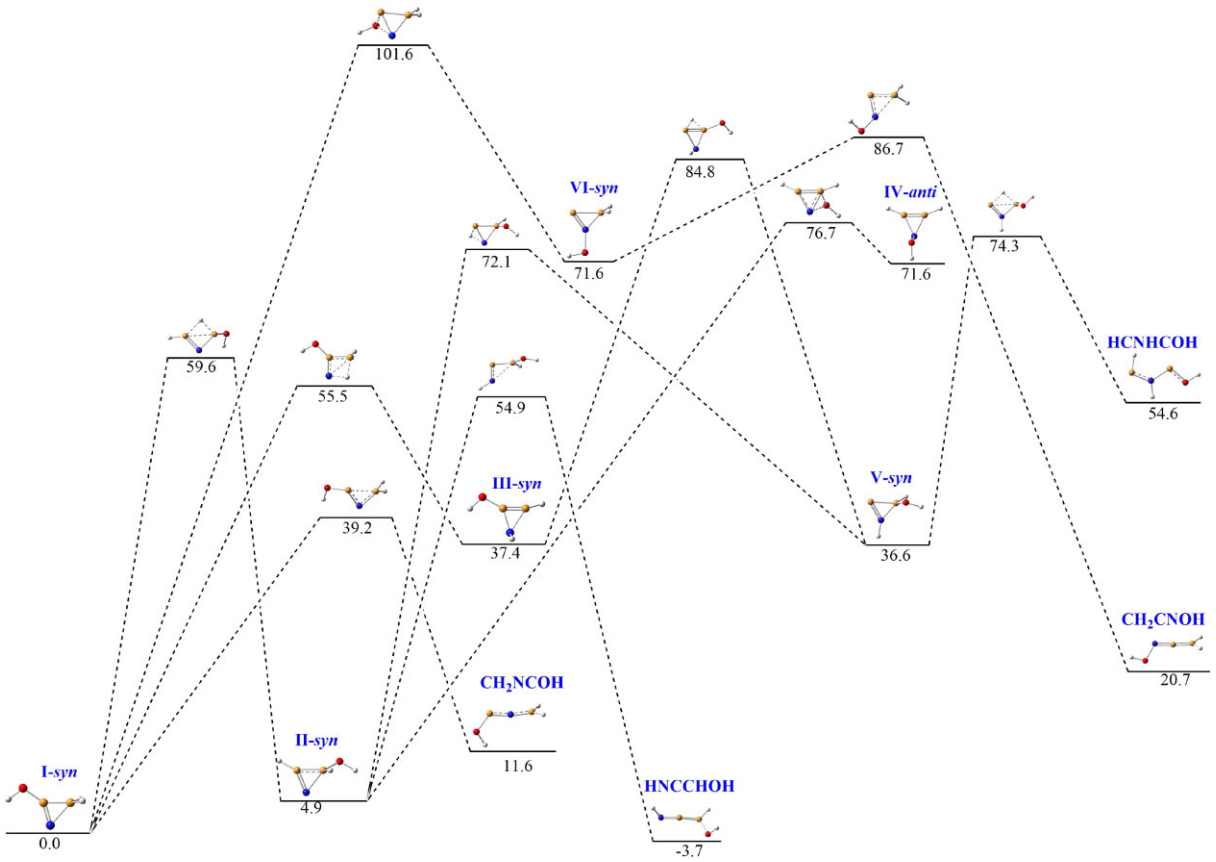

Figure 3. Energy profile for the isomerization processes between hydroxy-azirine isomers. Relative energies, in kcal/mol, are calculated with respect to *syn*-3-hydroxy-2H-azirine (I-*syn*) at the B2PLYPD3/aug-cc-pVTZ level. ZPV energies are included.

Table 6. Rotational (Q_r) and vibrational (Q_v) partition functions of *syn*-3-hydroxy-2H-azirine.

Temperature (K)	Q_r	Q_v
9.38	448.5	1.00
18.75	1262.2	1.00
37.50	3560.9	1.00
75.00	10058.9	1.00
150.00	28433.0	1.07
225.00	52223.7	1.30
300.00	80395.2	1.74

Table 7. Rotational (Q_r) and vibrational (Q_v) partition functions of *anti*-3-hydroxy-2H-azirine.

Temperature (K)	Q_r	Q_v
9.38	450.8	1.00
18.75	1268.7	1.00
37.50	3579.5	1.00
75.00	10111.6	1.00
150.00	28582.0	1.05
225.00	52497.4	1.25
300.00	80816.5	1.64

uncertainty in the frequency scale of ∼5.4 MHz for *a*-type *R*-branch transitions of the I-*syn* conformer. Within this framework, although we forecast a non-negligible uncertainty in the calculated rotational rest frequencies, we can use high-level predicted HPS patterns as a key spectroscopic motif to experimentally characterize and identify these N-containing molecules.

Afterwards, to obtain reliable line intensities, in Tables 6 and 7 we give the rotational (Q_r) and vibrational (Q_v) partition functions of conformers I-*syn* and I-*anti* (the most stable structures), respectively, which are mandatory to perform an eventual radio astronomical search. We employed SPCAT (Pickett 1991) to estimate the values of Q_r from first principles at the conventional temperatures as implemented in the JPL database (Pickett et al. 1998) using the ab initio predicted spectroscopic parameters reported in Table 5 and equation (3.67) of (Gordy & Cook 1970) as:

$$Q_r = \sum_{i=0}^{\infty} (2J+1) e^{-E_i/kT_{ex}} \tag{5}$$

In this case, the values of the rotational partition function were multiplied by the nuclear spin statistics contribution ($Q_n = 3$ due to the existence of a ^{14}N nucleus). Furthermore, we considered all the vibrational modes and estimated the vibrational part, Q_v, using an anharmonic approximation and the following expression (Gordy & Cook 1970):

$$Q_{\rm v} = \prod_{i=1}^{3N-6} \frac{1}{1 - e^{-E_i/kT_{\rm ex}}} \tag{6}$$

Table 8. Harmonic, ω, and anharmonic, ν, vibrational frequencies (cm^{-1}) and IR intensities (km/mol), for the 3-hydroxy-2H-azirine and 2-hydroxy-2H-azirine conformers calculated at the CCSD(T)/aug-cc-pVTZ level.

	syn-3-hydroxy-2H-azirine				*anti*-3-hydroxy-2H-azirine				*syn*-2-hydroxy-2H-azirine[a]				*anti*-2-hydroxy-2H-azirine[a]			
Mode	ω	I_{har}	ν	I_{anhar}	ω	I_{har}	ν	I_{anhar}	ω	I_{har}	ν	I_{anhar}	ω	I_{har}	ν	I_{anhar}
a", a	398	28.2	401	38.3	380	85.9	365	97.0	265	132.2	222	115.8	233	98.6	178	86.9
a', a	418	31.8	411	27.2	418	0.0	410	0.1	452	29.0	440	26.3	470	15.4	457	14.7
a", a	529	91.4	508	80.3	469	18.3	457	7.1	490	5.5	480	5.0	476	2.4	470	1.1
a', a	635	31.1	609	34.8	647	7.2	620	6.6	754	19.8	731	17.6	752	19.4	724	17.8
a', a	933	48.0	997	2388.0	930	86.4	900	14.4	802	20.0	790	15.9	797	21.2	787	19.3
a", a	964	0.6	947	0.4	962	0.3	933	0.3	994	18.4	971	20.2	972	58.7	952	55.1
a', a	1047	15.9	1022	9.4	1036	17.6	1007	15.9	1025	3.7	1005	9.0	1042	4.5	1009	4.7
a", a	1093	0.3	1076	0.3	1091	0.6	1071	0.6	1098	107.6	1069	116.5	1089	157.7	1060	154.5
a', a	1212	117.1	1188	114.3	1221	51.1	1193	50.6	1237	142.9	1193	1292.7	1273	7.6	1300	1656.8
a', a	1499	13.7	1464	6.7	1449	162.6	1405	34.7	1334	2.7	1303	3.8	1333	19.5	1297	20.2
a', a	1514	2.5	1476	1.2	1511	0.8	1469	1.5	1440	9.8	1454	**	1436	76.3	1394	1.6
a', a	1849	202.1	1798	47.9	1879	150.1	1851	22.5	1657	21.7	1624	18.6	1633	29.6	1603	25.5
a', a	3110	17.4	2994	16.5	3104	17.9	2988	16.5	3151	21.3	3025	18.2	3194	5.6	3059	6.1
a", a	3200	12.1	3052	15.8	3193	14.0	3042	17.9	3223	0.2	3083	0.9	3203	4.8	3062	7.8
a', a	3747	61.9	3561	49.3	3817	104.8	3631	88.6	3811	45.8	3624	35.3	3812	36.4	3628	29.3

Note.[a] Anharmonic contributions are computed at the CCSD(T)/cc-pVTZ level.

The total partition function (Q_{tot}) can be obtained as the product of Q_r and Q_v. Note that for those astronomical sources where a Boltzmann distribution can be assumed for the target species, an additional conformational correction factor will be needed to derive a proper estimation of the total column density (upper limit) of each hydroxy-azirine conformer. The harmonic, ω, and anharmonic, ν, vibrational frequencies and IR intensities of the most stable hydroxy-azirine structures, computed at the CCSD(T)/aug-cc-pVTZ level, are given in Table 8. Hence, these parameters can be confidently used to model a reliable IR spectrum and to guide, eventually, an experimental characterization using IR spectroscopy.

At a final step, to generate predictions of their rotational spectra, we employed the *S*-reduced form of an asymmetric Hamiltonian in the I^r representation ($H_R^{(A)}$) (Watson 1977), augmented with a term (H_Q) that accounts for the nuclear quadrupole interaction ($H = H_R^{(A)} + H_Q$) (Foley 1947; Robinson & Cornwell 1953). The energy levels involved in each transition and related to the hyperfine structure are labeled with the quantum numbers J, K_a, K_c, and F, where, $F = I + J$, since the rotational Hamiltonian is assembled in the coupled basis set. As can be seen in Fig. 4(a), for conformer I-*syn* the spectral search should be directed toward the identification of intense and characteristic *a*-type *R*-branch transitions, which are spaced by approximately $B + C$ and should be easily recognized in the spectra. On the contrary, *b*-type *R*-branch lines shall be the primary target for conformer I-*anti* due to its higher predicted *b*-type dipole moment component ($|\mu_b| = 3.5$ D). Moreover, although the brightest lines for these species fall off the Q-band (they are located at ∼3 mm), the HPS represents an essential piece of information for centimeter-wave observations since low J rotational transitions exhibit their hyperfine components spread over several hundreds of kHz or even few MHz [see the insets of Fig. 4(a and b)]. This fact further motivates radio astronomers to search for these astrophysically relevant molecules using low-frequency surveys (i.e. those conducted in the Q-band). Additionally, for astrophysical purposes, we provide a complete list of the predicted lines (∗.cat files) including the HPS for both I-*syn* and I-*anti* conformers as Supplementary Material (online).

In summary, the theoretical spectroscopic information here provided will be essential to accomplish an eventual laboratory detection. Additionally, these data can be used to perform a fledgling insterstellar search for hydroxy-azirine using different astronomical data sets performed at cm-wavelengths, such as the GBT GOTHAM (Green Bank Telescope Observations of TMC-1: Hunting Aromatic Molecules) survey (Siebert et al. 2022) and the Yebes 40 m QUIJOTE line survey (Cernicharo et al. 2022) (both conducted toward the cold dark cloud TMC-1), and the Yebes 40 m survey toward the G + 0.693-0.027 molecular cloud (Jiménez-Serra et al. 2022). In this context, G + 0.693-0.027, located in Galactic Centre region, appears as one of the most promising astronomical sources to search for these prebiotic molecules, given the increasing level of molecular complexity found toward this molecular cloud over the last few years (Rivilla et al. 2020, 2021a,b; Rodríguez-Almeida et al. 2021; Jiménez-Serra et al. 2022).

3.4 Some insights into the formation of hydroxy azirine in interstellar medium

We will study the possibility of the formation of hydroxy-azirine from 2H-azirine, considering that this molecule is likely to be present in the ISM. Recently ethynyl cyclopropenylidene (c-C_3HC_2H) has been identified in the interstellar medium (Cernicharo et al. 2021d) and theoretical studies have proposed the formation of monosubstituted cyclopropenylidene derivatives through gas-phase additions of X onto c-C_3H_2 (being X a radical, such as CN, OH, F, or NH_2) (Fortenberry 2021; Flint & Fortenberry 2022). In a similar way, the formation of the detected benzonitrile (McGuire et al. 2018) and cyanocyclopentadiene (McCarthy et al. 2021) from the reaction between CN radical and benzene or cyclopentadiene have been proposed (Cooke et al. 2020; McCarthy et al. 2021) as possible ways of formation. In this regard, we have considered the gas phase reaction between OH and 2H-azirine as a potential generation route of hydroxy azirine.

As we have mentioned in Section 1, 2H-azirine has also been proposed to be formed in ices (Turner & Apponi 2001; Kuan et al. 2004). Thus, we have also studied its possible formation on icy surfaces. For this purpose, the surface effect, as a first approximation, has been taken into account by considering the 2H-azirine molecule adsorbed on one or two water molecules. In a previous work (Redondo et al. 2021), we have seen that modeling the surface with two water molecules gives results close to those obtained considering larger cluster or solid-state approaches.

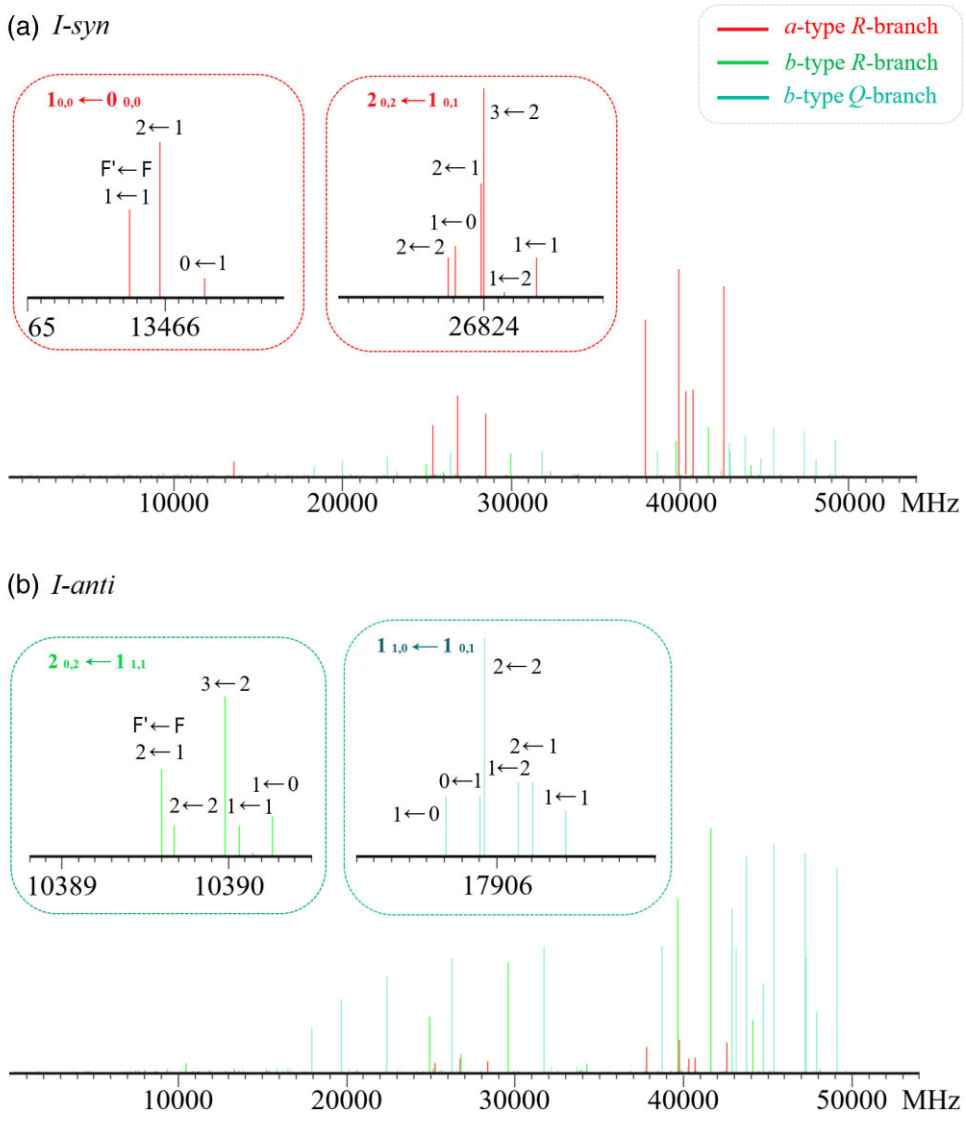

Figure 4. a) Predicted synthetic rotational spectrum of the I-*syn* conformer of hydroxy-azirine at 10 K in the 0-50 GHz frequency range, calculated from the theoretical spectroscopic parameters presented in Table 5; an inset showing the HPS of the $1_{0,0} \leftarrow 0_{0,0}$ and $2_{0,2} \leftarrow 1_{0,1}$ transitions is also included. b) Predicted synthetic rotational spectrum of the I-*anti* conformer at 10 K in the 0-50 GHz frequency range, computed from the theoretical spectroscopic parameters listed in Table 5; a zoomed view showing the HPS of the $2_{0,2} \leftarrow 1_{1,1}$ and $1_{1,0} \leftarrow 1_{0,1}$ transitions is also included.

The reaction profile for the reaction between 2H-azirine and OH in the gas phase and in presence of two H_2O molecules is shown in Fig. 5, and the energy of the stationary points located on the potential energy surface considering gas phase, 1 and 2 H_2O molecules are given in Table 9. The geometry optimizations and frequencies have been obtained at the B2PLYPD3/aug-cc-pVTZ level and the energies have been also calculated at the CCSD(T)-F12/cc-pVTZ-F12 level. As can be seen in Fig. 5, the reaction starts by the formation of an intermediate I1, which is a complex between OH and 2H-azirine. From I1, the insertion of the OH radical to the carbon bonded with one hydrogen atom, forming the intermediate denoted as I2 through the transition state TS1. Once the intermediate I2 has been reached, the elimination of the H atom from the carbon bonded to the oxygen (*path a*) leads to the formation of *syn*-3-hydroxy-2H-azirine (I-*syn*); this process involves the transition state TS2. If one of the hydrogens of the other carbon is removed from I2 (*path b*), the isomer *syn*-2-hydroxy-2H-azirine (II-*syn*) is obtained by passing through the transition state TS3. The reaction paths can be summarized as:

2H-azirine + OH → *I*1 → TS1 → *I*2 → TS2 → I-*syn* + H *path a*
2H-azirine + OH → *I*1 → TS1 → *I*2 → TS3 → II-*syn* + H *path b*

When the reaction takes place in gas phase, the formation of the isomer *syn*-3-hydroxy-2H-azirine is an exothermic process, whereas the formation of *syn*-2-hydroxy-2H-azirine is *quasi* isoenergetic, as can be seen in Table 9. Although from a thermodynamic point of view the formation of both products could be viable; however, the two processes involve a net activation barrier since the hydrogen elimination transition states, TS2 and TS3 are located 3.48 and 3.52 kcal/mol above the reactants at the CCSD(T)-F12/cc-pVTZ-F12 level, respectively. Therefore, the formation of hydroxy azirine from the gas-phase reaction of 2H-azirine with OH would not be feasible in the conditions of the interstellar medium. If the reaction starts from 2H-azirine adsorbed on 1 or 2 H_2O molecules, then both products I-*syn* and II-*syn* are clearly exothermic and the reaction proceeds with

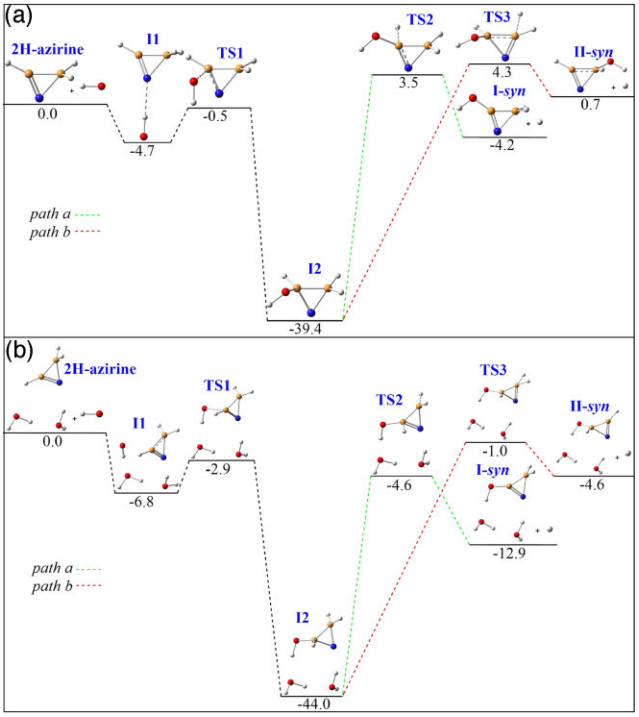

Figure 5. Reaction profiles for the reaction between 2H-azirine and OH calculated at the CCSD(T)-F12/cc-pVTZ-F12 level. (a) In gas phase and (b) in presence of two H_2O molecules. Relative energies in kcal/mol (ZPV energies includes).

no net activation barrier; all the transition states are located below the reactants (see Table 9 and Fig. 5). Therefore, the formation of hydroxy azirine from 2H-azirine would be a viable process in the interstellar medium if it takes place on the surface of ices.

4 CONCLUSIONS

We have carried out a state-of-the-art theoretical study on the possible interstellar species hydroxy-azirine (c-C_2H_3NO), which can be seen as a functionalized derivative of the nitrogen-containing three-membered cycle azirine (C_2H_3N), where a hydrogen atom is replaced by a -OH unit. For each family of isomers, derived from 2H-azirine, 1H-azirine, and the carbene isomer, we have characterized two distinct structural isomers, each of which presents two conformers, denoted as *syn*- and *anti*-, that account for the different orientation of the -OH group. The characterization of the 12 structures was initially performed at the B2PLYPD3/aug-cc-pVTZ and CCSD(T)/cc-pVTZ-F12 levels. Very close results were obtained at both calculation levels.

The structures derived from the most stable azirine isomer, 2H-azirine, are also the most stable ones and appear as the most promising targets to be detected experimentally, both in the laboratory and in the ISM. The 3-Hydroxy-2H-azirine isomer in its *syn*- conformation (I-*syn*) is the lowest-lying structure with the *anti*-conformer (I-*anti*) located only 1.21 kcal/mol above I-*syn* at the CCSD(T)-F12/cc-pVTZ-F12 level. The next isomer in stability is 2-hydroxy-2H-azirine (II), the *syn*- and *anti*-conformers lie 3.86 and 4.26 kcal/mol above the I-*syn* isomer at the CCSD(T)-F12/cc-pVTZ level, respectively. The remaining isomers are located more than 30 kcal/mol above the I-*syn* isomer. In general, we found that isomers arising from the carbene-like azirine isomer, and H-azirine, where the hydroxyl is attached to the carbon atom, are much more stable than those where the attachment is conducted on the nitrogen one. As in azirine, the isomers belonging to the carbene family are more stable than those derived from 1H-azirine when the OH substitution takes place at the carbon atom, but if the substitution is performed at the nitrogen atom the order is reversed.

We have analysed the isomerization processes between the different hydroxy-azirine structures, including also the cleavage of the cycle to form open-chain species. Net activation barriers were found for all processes and, therefore, interconversion between isomers would not be possible in the interstellar medium. Moreover, if viable formation pathways existed the different isomers could be present. We have also determined the interconversion barriers between conformers. A barrier of 5.17 kcal/mol (≈2600 K) (CCSD(T)-F12/cc-pVTZ-F12 level) is found for the most stable isomer, 3-hydroxy-2H-azirine (I). Therefore, both conformers can be identified experimentally, both in the laboratory and in the ISM. For the isomer, 2-hydroxy-2H-azirine (II), a barrier of 0.25 kcal/mol (≈125 K) (CCSD(T)-F12/cc-pVTZ-F12 level) is obtained, indicating that both *syn*- and *anti*-conformers could be present in low-temperature interstellar clouds, but in a conventional rotational experiment the II-*anti* conformer shall interconvert into the II-*syn* conformer, precluding its detection.

For the four most stable isomers: I-*syn*, I-*anti*, II-*syn,* and II-*anti*, which are the most interesting from an experimental point of view, we have applied composite methods, which allowed us to obtain very accurate theoretical spectroscopic parameters, needed to interpret their rotational spectra. Moreover, for astronomical purposes, we provide a prediction of the rest frequencies up to 50 GHz (including the HPS structure) along with the rotational and vibrational partition functions for the I-*syn* and I-*anti* conformers. Anharmonic vibrational frequencies and intensities, which are mandatory to model

Table 9. Stationary points for the reaction between 2H-azirine and OH in gas phase and in presence the one or two water molecules. Energy differences in kcal/mol calculated at the B2PLYPD3/aug-cc-pVTZ and CCSD(T)-F12/cc-pVTZ-F12 levels (ZPV energies included).

	Gas phase		1-H_2O molecule		2-H_2O molecule	
	B2PLYPD3	CCSD(T)-F12	B2PLYPD3	CCSD(T)-F12	B2PLYPD3	CCSD(T)-F12
2H-azirine + OH	0.00	0.00	0.00	0.00	0.00	0.00
I1	−4.67	−4.73	−6.51	−6.28	−6.76	−6.84
I2	−39.41	−39.60	−42.09	−42.67	−44.00	−43.97
TS1	−0.49	−0.15	−2.58	−2.70	−3.59	−2.94
TS2	3.47	3.48	−2.58	−2.70	−5.50	−4.61
TS3	4.28	3.52	1.92	0.68	−0.47	−0.90
I-*syn* + H	−4.17	−4.13	−9.42	−9.49	−13.69	−12.92
II-*syn* + H	0.71	−0.32	−1.54	−3.04	−3.80	−4.57

a reliable theoretical vibrational spectra, are also reported at the CCSD(T)/aug-cc-pVTZ level.

Finally, we have studied the formation of hydroxy-azirine from the reaction between 2H-azirine and the OH radical. Our results show that, the gas-phase reaction will not be feasible under the conditions of the interstellar medium. However, if the reaction takes place starting from 2H-azirine adsorbed on 1 or 2 H_2O molecules, the formation of *syn*-3-Hydroxy-2H-azirine and *syn*-2-Hydroxy-2H-azirine are clearly exothermic processes and barrier free. Thus, the formation of hydroxy-azirine from 2H-azirine would be a viable process on the surface of interstellar ices, further supporting its interest as appealing astronomical candidate.

ACKNOWLEDGEMENTS

Financial support from the Spanish Ministerio de Ciencia e Innovación (PID2020-117742GB-I00) and Junta de Castilla y Leon (Grant VA244P20) is gratefully acknowledged.

DATA AVAILABILITY

The main data underlying this article are available in the article and in its online supplementary material. Additional data will be shared on reasonable request to the corresponding author.

REFERENCES

Alessandrini S., Gauss J., Puzzarini C., 2018, J. Chem. Theory Comput., 14, 5360
Apponi A. J., McCarthy M. C., Gottlieb C. A., Thaddeus P., 1999, ApJ, 516, L103
Barnum T. J. et al., 2022, J. Phys. Chem. A, 126, 2716
Belloche A. et al., 2017, A&A, 601, A49
Cernicharo J., Agúndez M., Kaiser R. I., Cabezas C., Tercero B., Marcelino N., Pardo J. R., de Vicente P., 2021a, A&A, 655, L1
Cernicharo J., Agúndez M., Kaiser R. I., Cabezas C., Tercero B., Marcelino N., Pardo J.R., de Vicente P., 2021b, A&A, 652, L9
Cernicharo J., Cabezas C., Endo Y., Agúndez M., Tercero B., Pardo J. R., Marcelino N., de Vicente P., 2021c, A&A, 650, L14
Cernicharo J., Agúndez M., Cabezas C., Tercero B., Marcelino N., Pardo J.R., de Vicente P., 2021d, A&A, 649, L15
Cernicharo J., Fuentetaja R., Agúndez M. et al., 2022, A&A, 663, L9
Cooke I. R., Gupta D., Messinger J. P., Sims I. R., 2020, ApJ, 891, L41
Csaszar A. D., Demaison J., Rudolph H. D., 2015, J. Phys. Chem. A, 119, 1731
Dickens J. E., Irvine W. M., Ohishi M., Ikeda M., Ishikawa S., Nummelin A., Hjalmarson Å., 1997, ApJ, 489, 753
Dickens J. E., Irvine W. M., Nummelin A. et al., 2001, Spectrochimica Acta Part A, 57, 643 A
Dickerson C. E., Bera P. P., Lee T. J., 2018, J. Phys. Chem. A, 122, 8898
Dunning T. H., 1989, JChPh, 90, 1007
Flint A. R., Fortenberry R. C., 2022, ApJ, 938, 15
Foley H. M., 1947, Phys. Rev., 71, 747
Fortenberry R. C., 2021, ApJ, 921, 132
Frisch M. J. et al., 2016, Gaussian 16, Revision B + 01. Gaussian, Wallingford, CT, USA
Gardner M. B., Westbrook B. R., Fortenberry. R. C., Lee T. J., 2021, Spectrochimica Acta Part A: Molecular and Biomolecular Spectroscopy, 248, 119184
Gordy W., Cook R. L., 1970, Microwave Molecular spectra. Interscience Pub, New York
Gottlieb C. A., 1973, in Gordon M. A., Snyder L. E., eds, Molecules in the Galactic Environ-ment. Wiley-Interscience, New York, p. 181
Grimme S. J., 2006, ChPh, 124, 034108
Grimme S., Ehrlich S., Goerigk L., 2011, J. Comp. Chem., 32, 1456
Halfen D. T., Ilyushin V. V., Ziurys L. M., 2015, ApJ, 812, L5
Helgaker T., Klopper W., Koch H., Noga J., 1997, JChPh, 106, 9639
Jiménez-Serra I., Rodríguez-Almeida L. F., Martín-Pintado J. et al., 2022, A&A, 663, A181
Knizia G., Adler T. B., Werner H.-J., 2009, JChPh, 130, 054104
Kuan Y.-J., Charnley S. B., Huang H.-C., Kisiel Z., Ehrenfreund P., Tseng W.-L., Yan C.-H., 2004, Adv. Space Res., 33, 31
Kutner M. L., Machnik D. E., Tucker K. D., Dickman R. L., 1980, ApJ, 242, 541
Lattelais M., Pauzat F., Ellinger Y., Ceccarelli C., 2009, ApJ, 696, L133
Lee T. J., Taylor P. R., 1989, Int. J. Quant. Chem. Symp., S23, 199
Lee K. L. L. et al., 2021, ApJ, 910, L2
Loomis R. A. et al., 2021, Nat. Astron., 5, 188
Martins Z., 2018, Life (Basel), 8, 28
McCarthy M. C. et al., 2021, Nat. Astron., 5, 176
McGuire B. A., 2022, ApJS, 259, 30
McGuire B. A., Carroll P. B., Loomis R. A., Finneran I. A., Jewell P. R., Remijan A. J., Blake G. A., 2016, Science, 352, 1449
McGuire B. A., Burkhardt A. M., Kalenskii S., Shingledecker C. N., Remijan A. J., Herbst E., McCarthy M. C., 2018, Science, 359, 202
Menor-Salván C., Marín-Yaseli M. R., 2012, Chem. Soc. Rev., 41, 5404
Miller T. F., Clary D. C., Meijer A. J. H. M., 2005, J. Chem. Phys., 122, 244323
Mills I. M., 1972, in Rao K. N., Mathews C. W., eds, Vibration-Rotation Structure in Asymmetric and Symmetric-Top Molecules. In Molecular Spectroscopy: Modern Research. Academic Press, New York, p. 115
Peeters Z., Botta O., Charnley S. B. R. , Ruiterkamp R., Ehrenfreund P., 2003, ApJ, 593, L129
Peeters Z., Botta O., Charnley S. B., Kisiel Z., Kuan Y.-J., Ehrenfreund P., 2005, A&A, 433, 583
Peterson K. A., Adler T. B., Werner H. J., 2008, JChPh, 128, 084102
Pickett H. M., 1991, J. Mol. Spectrosc., 148, 371
Pickett H. M., Poynter R. L., Cohen E. A., Delitsky M. L., Pearson J. C., Müller H. S. P., 1998, J. Quant. Spec. Radiat. Transf., 60, 883
Raghavachari K., Trucks G. W., Pople J. A., Head-Gordon M., 1989, CPL, 157, 479
Redondo P., Martínez H., Largo A., Barrientos C., 2017, A&A, 603, A139
Redondo P., Largo A., Barrientos C., 2018, MNRAS, 478, 3042
Redondo P., Sanz-Novo M., Largo A., Barrientos C., 2020, MNRAS, 492, 1827
Redondo P., Pauzat F., Markovits A., Ellinger Y., 2021, A&A, 646, A163
Rivilla V. M. et al., 2020, ApJ, 899, L28
Rivilla V. M. et al., 2021a, Proc. Natl. Acad. Sci., 118, 2101314118
Rivilla V. M. et al., 2021b, MNRAS, 506, L79
Robinson G. W., Cornwell C. D., 1953, J. Chem. Phys., 21, 1436
Rodriguez L. E., House C. H., Smith K. E., Roberts M. R., Callahan M. P., 2019, NatSR, 9, 9281
Rodríguez-Almeida L. F. et al., 2021, A&A, 654, L1
Ruoff R. S., Klots T. D., Emilsson T., Gutowsky H. S., 1990, J. Chem. Phys., 93, 3142
Schwartz A. W., Joosten H., Voet A., 1982, Biosystems, 15, 191
Siebert M. A., Lee K. L. K., Remijan A. J., Burkhardt A. M., Collaboration The GOTHAM, Loomis R. A., McCarthy M. C., McGuire B. A., 2022, ApJ, 924, 21
Stanton J. F., Gauss J., Cheng L., Harding M. E., Matthews D.A., Szalay P. G., 2019, CFOUR, A Quantum Chemical Program. Package http://www.cfour.de/ureference
Tavakol H., 2010, J. Mol. Struct.: THEOCHEM, 956, 97
Thaddeus P., Cummins S. E., Linke R. A., 1984, ApJ, 283, L45
Turner B. E., Apponi A. J., 2001, ApJ, 561, L207
Turner A. M., Chandra S., Fortenberry R. C., Kaiser R. I., 2021, ChemPhysChem, 22, 985
Watson J. K., 1968, MPh., 196815, 479
Watson J. K. G., 1977, in During J., ed., Vibrational Spectra and Structure, Vol. 6, ch. 1. Elsevier, Amsterdam
Werner H.-J. et al., 2019, MOLPRO, version 2020.1, a package of ab initio programs, https://www.molpro.net
Woon D. E., Dunning T. H., 1993, JChPh, 98, 1358

Zeng S., Quénard D., Jiménez-Serra I., Martín-Pintado J., Rivilla V. M., Testi L., Martín-Doménech R., 2019, MNRAS, 484, L43

SUPPORTING INFORMATION

Supplementary data are available at *MNRAS* online.

SI-Geometries-frequencies-OH-azirine.pdf
I-anti-300K.cat
I-syn-300K.cat

Please note: Oxford University Press is not responsible for the content or functionality of any supporting materials supplied by the authors. Any queries (other than missing material) should be directed to the corresponding author for the article.

This paper has been typeset from a TEX/LATEX file prepared by the author.